Bioorganic & Medicinal Chemistry Letters 20 (2010) 1378–1383

Contents lists available at ScienceDirect

Bioorganic & Medicinal Chemistry Letters

journal homepage: www.elsevier.com/locate/bmcl

Structure–activity relationships of diphenylpiperazine N-type calcium channel inhibitors

Hassan Pajouhesh [a], Zhong-Ping Feng [a,b,†], Yanbing Ding [a], Lingyun Zhang [a], Hossein Pajouhesh [a], Jerrie-Lynn Morrison [a], Francesco Belardetti [a], Elizabeth Tringham [a], Eric Simonson [a], Todd W. Vanderah [c], Frank Porreca [c], Gerald W. Zamponi [b], Lester A. Mitscher [d], Terrance P. Snutch [e,*]

[a] Neuromed Pharmaceuticals Ltd, 301-2389 Health Sciences Mall, Vancouver, BC, Canada
[b] Department of Physiology and Pharmacology, University of Calgary, Calgary, AB, Canada
[c] Department of Pharmacology, University of Arizona, Tucson, AZ, USA
[d] Department of Medicinal Chemistry, University of Kansas, Lawrence, KS, USA
[e] Michael Smith Laboratories, University of British Columbia, Vancouver, BC, Canada

ARTICLE INFO

Article history:
Received 24 September 2009
Revised 27 December 2009
Accepted 4 January 2010
Available online 7 January 2010

Keywords:
Calcium channel
N-type
L-type
Pain
Diphenylpiperazine

ABSTRACT

A novel series of compounds derived from the previously reported N-type calcium channel blocker **NP118809** (1-(4-benzhydrylpiperazin-1-yl)-3,3-diphenylpropan-1-one) is described. Extensive SAR studies resulted in compounds with IC_{50} values in the range of 10–150 nM and selectivity over the L-type channels up to nearly 1200-fold. Orally administered compounds **5** and **21** exhibited both anti-allodynic and anti-hyperalgesic activity in the spinal nerve ligation model of neuropathic pain.

Numerous neuronal functions including neurotransmitter release, excitability and gene expression are highly dependent upon of the activity of voltage-gated calcium channels. Of the L-, N- and P/Q-types of native high voltage-gated calcium channels in neurons, the N-type channel exhibits a variety of characteristics suitable for therapeutic interventions aimed at relieving chronic and neuropathic pain conditions. In the dorsal horn of the spinal cord, $Ca_V2.2$ (α_{1B}) subunits encoding the N-type channel are concentrated at presynaptic terminals where they play a prominent role in triggering the release of the pain-related transmitters glutamate, CGRP and substance P.[1] N-type channels are also a target for modulation by a number of G-protein coupled receptors including the mu-opioid receptor-mediated inhibition that acts to attenuate transmitter release via a G-protein-dependent mechanism.[2] The cone snail peptide, ω-conotoxin-MVIIA (Ziconotide®, Prialt™), reversibly blocks N-type channels, inhibits the release of substance P and CGRP, and is highly efficacious towards alleviating inflammatory and neuropathic pain in both animals and humans.[3] While both US and European regulatory agencies have approved the use of Prialt™ for the treatment of intractable pain, it must be delivered intrathecally and is not without adverse effects.[4]

A number of groups have focused on development of non-peptidic based small molecule N-type calcium channel blockers aimed at treating inflammatory and chronic pain.[5] We recently reported **NP118809** (Fig. 1) as a potent N-type calcium channel blocker with ~110-fold selectivity over the L-type calcium channel and good efficacy in a rodent model of inflammatory pain.[6] As part of our effort to further optimize the development of orally available N-type calcium channel blockers, we tested aryl substitutions on the benzhydryl moiety bound to the piperazine core of **NP118809** (Table 1) and also examined a bioisosteric series (Table 2). Subsequently, we

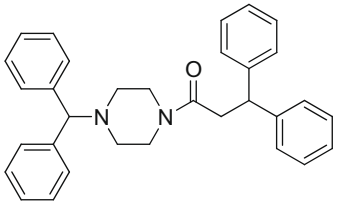

Figure 1. Structure of **NP118809**.

* Corresponding author. Tel.: +1 604 822 6968; fax: +1 604 822 6470.
E-mail address: snutch@msl.ubc.ca (T.P. Snutch).
† Present Address: Department of Physiology, University of Toronto, Toronto, ON, Canada.

0960-894X/$ - see front matter © 2010 Elsevier Ltd. All rights reserved.
doi:10.1016/j.bmcl.2010.01.008

Table 1
N-type and L-type calcium channel blocking activities for compounds **1–20**

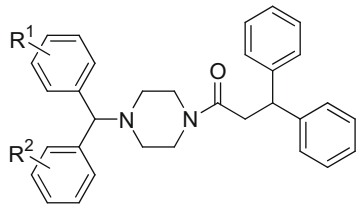

Compound	R^1	R^2	N-type Est. IC_{50} (μM)	L-type Est. IC_{50} (μM)	L-type FLIPR IC_{50} (μM)
NP118809	H	H	0.11	12.2	
1	*para*-CF_3	H	0.07	19.6	6.1
2	*meta*-CF_3	H	0.11	6.6	1.8
3	*ortho*-CF_3	H	0.30		10
4 (Racemate)	*para*-Cl	H	0.11		7.4
5 (*R*-Isomer)	*para*-Cl	H	0.05	4.3	6.9
6 (*S*-Isomer)	*para*-Cl	H	0.14		6.8
7	*meta*-Cl	H	0.04	8.5	6.2
8	*ortho*-Cl	H	0.09	106	>10
9	*para*-F	H	0.38		1.1
10	*para*-CH_3	H	0.31		2.5
11	*para*-OCH_3	H	0.25		1.6
12	*para*-OCH_3	p-OCH3	0.24		2.9
13	3,4,5-Tri-OCH_3	H	0.51		1.4
14	3,5-Di-Cl	H	0.17		≫10
15	2,6-Di-Cl	H	0.21		≫10
16	2,3-Di-Cl	H	0.22		>10
17	2,4-Di-Cl	H	>1		≫10
18	3,4-Di-Cl	H	>1		>10
19	2,4-Di-CH_3	H	0.23		9.6
20	3,5-Di-OCH3	H	0.21		—

The N-type and L-type IC_{50} columns indicate estimated IC_{50} values as determined by whole-cell patch clamp of transiently expressed calcium channel complexes. For the L-type FLIPR-based assay IC_{50} values were calculated from an 8 point concentration-dependent response profile for each compound (0.003–10 μM). In those instances wherein the highest concentration (10 μM) resulted in incomplete blockade we indicate >10: 10–50% inhibition at 10 μM and ≫10 μM: less than 10% inhibition at 10 μM.

sequentially substituted heterocycles for the aryl group on the benzhydryl moiety (Table 4).

The synthesis of compounds with the targeted substitution changes is described in Scheme 1. The starting material diphenylmethanols were synthesized as described in the literature.[7] Treatment with thionyl chloride, followed by coupling with Boc-piperazine, provided a benzhydrylpiperazine that was transformed into product upon reaction with 3,3-diphenylpropionic acid and diphenylmethyl isocyanate. Some experimental details have been published in patent form.[8]

The structure–activity analyses of the various chemical series were guided by manual whole-cell patch clamp electrophysiological assay of rat neuronal N-type[9] and L-type[10] channels expressed in HEK cells (N-type: $\alpha_{1B}/Ca_V2.2 + \alpha_2\delta\text{-}1 + \beta_{1b}$ subunits; L-type: $\alpha_{1C}/Ca_V1.2 + \alpha_2\delta\text{-}1 + \beta_{1b}$ subunits). Whole-cell barium currents were elicited from a holding potential of −100 mV to the peak of the current–voltage relation for each channel type.[11] Each compound was examined for inhibition on 3–5 cells. A FLIPR cell-based functional assay also was used to characterize the block of L-type voltage-dependent calcium channels in the partially inactivated state.[12] The basis of this assay is measurement in plate format of calcium influx through a stably expressed L-type calcium channel complex ($\alpha_{1C}/Ca_V1.2 + \alpha_2\delta + \beta_2a$ subunits) in response to potassium-mediated depolarization. This cell line was also stably transfected with the Kir2.3 inward rectifier K^+ channel which allows for changing the cell membrane potential by modulation of extracellular $[K^+]_o$ containing buffer. Table 1 illustrates the structure–activity trend in N-type inhibition for mono- versus di-substituted phenyl on the diphenylmethylene. Compounds with a single electron-withdrawing substituent on one of the phenyl groups are highly potent N-type channel blockers (compounds **1–9**). N-type blocking affinity does not appear to depend upon either the exact nature of the electron-withdrawing substituent (CF_3, Cl, F) or its position on the phenyl ring (Table 1). For example, compare compound **1**, where the trifluoromethyl is at the *para*-position with compounds **7** and **8** where the chlorine is at the *meta*- and *ortho*-positions, respectively. In addition to possessing high N-type blocking activities, this series exhibited a high degree of selectivity over the neuronal L-type calcium channel (~60–1178-fold).

When matched pairs at the *para*-position are compared (Table 1), the methyl- and methoxy-substituted phenyl compounds (**10** and **11**) are consistently less potent N-type blockers than their chloro- and trifluoromethyl counterparts (compounds **1** and **5**). These results suggest that electron-donating substituent groups have lower overall affinity for the N-type channel compared to that for compounds containing electron-withdrawing substituents.

As part of the structure–activity studies, the effects of di-substitutions on a single phenyl ring were also explored (Table 1). Compounds **14–16** illustrate that di-substitution with electron-withdrawing groups at the *ortho*- and *meta*-positions of the phenyl ring does not significantly affect N-type blocking affinity as compared to the single substituent analogues. However, when one of the electron-withdrawing substituents is at the *para*-position N-type blocking affinity is lost (compounds **17** and **18**).

Compounds **21–27** (Table 2) represent the N,4-dibenzhydryl-piperazine-1-carboxamide series (X=CO, Y=NH, Z=CH). The non-substituted derivative (compound **21**) showed a similar inhibitory activity for N-type calcium channels (est. IC_{50} = 0.15 μM) as that of parent compound, **NP118809**. However, this compound had a higher affinity for the L-type channel resulting in a comparatively lower L-type:N-type selectivity ratio (~12-fold). The substitution of a chlorine group at the 3-position of the benzhydryl moiety (compound **23**) led to a 2-fold decrease in N-type blocking activity compared to compound **21**, but a better overall L-type:N-type selectivity (~53-fold). Further analogues with di-substitution at the benzhydryl moiety did not show any overall improvement in

Table 2
N-type and L-type calcium channel blocking activities for compounds **21**–**41**

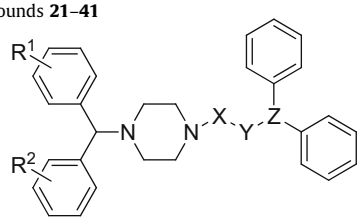

Compound	X	Y	Z	R^1	R^2	N-type Est. IC_{50} (μM)	L-type Est. IC_{50} (μM)	L-type FLIPR IC_{50} (μM)
NP118809	CO	NH	CH	H	H	0.11	12.2	—
21	CO	NH	CH	H	H	0.15	1.84	3.5
22	CO	NH	CH	H	2-Cl	0.18	0.61	>10
23	CO	NH	CH	H	3-Cl	0.34	17.9	>10
24	CO	NH	CH	H	4-Cl	0.28		>10
25	CO	NH	CH	H	2,3-Di-Cl	0.20		≫10
26	CO	NH	CH	H	2,4-Di-Cl	1.48	1.03	≫10
27	CO	NH	CH	H	2,4-Di-Me	2.71		>10
28	CO	CH	N	H	H	6.61		>10
29	CO	CH	N	H	2-Cl	0.32		>10
30	CO	CH	N	H	3-Cl	0.28		>10
31	CO	CH	N	H	4-Cl	0.50		>10
32	CO	CH	N	H	2,3-Di-Cl	0.14		>10
33	CO	CH	N	H	2,4-Di-Cl	0.46		≫10
34	CO	CH	N	H	2,4-Di-Me	0.26		≫10
35	CH	CO	N	H	H	0.26		1.6
36	CH	CO	N	H	2-Cl	0.05		1.1
37	CH	CO	N	H	3-Cl	0.32		1.4
38	CH	CO	N	H	4-Cl	0.11		2.9
39	CH	CO	N	H	2,3-Di-Cl	0.24		7.9
40	CH	CO	N	H	2,4-Di-Cl	0.51		8.6
41	CH	CO	N	H	2,4-Di-Me	1.25		3.8

The N-type and L-type IC_{50} columns indicate estimated IC_{50} values as determined by whole-cell patch clamp of transiently expressed calcium channel complexes. For the L-type FLIPR-based assay IC_{50} values were calculated from an 8 point concentration-dependent response profile for each compound (0.003–10 μM). In those instances wherein the highest concentration (10 μM) resulted in incomplete blockade we indicate >10: ~10–50% inhibition at 10 μM and ≫10 μM: less than 10% inhibition at 10 μM.

either N-type blocking affinity or in calcium channel selectivity (compounds **25**–**27**).

Replacement of the carboxamide in compounds **21** with the ethanone group (X=CO, Y=CH, Z=N) (compound **28**) showed a dramatic 44-fold decrease in N-type channel blocking activity (Table 2). Contrastingly, either mono- or di-substitution of one of the phenyl groups on the benzhydryl did not significantly affect N-type blocking affinity (compounds **29**–**34**). Further exploration of the structural activity relationship of derivatives focused around the **NP118809** linker moiety (X=CH, Y=CO, Z=N) resulted in compounds with a generally good degree of N-type channel inhibition (compounds **35**–**41**). Unlike that for compound **28**, these linker modifications (e.g., compound **35)** did not seem to be highly deleterious. The information from this series (**21**–**41**) may provide insight into the compound binding conformation at a site on the channel where slight alterations in the linker can have dramatic effect on N-type calcium channel activity.

Table 3
Aqueous kinetic solubility

Compound	pH 7.4 (μg/ml)
NP118809	0.52
2	0.14
4	0.23
5	0.13
6	0.16
7	0.37
8	0.37
21	0.38
43	63.6
45	41.0
46	72.7
49	151

The thermodynamic (equilibrium) solubility was determined using methodology based upon the OECD Water Solubility Method an LC/MS/MS system. Solubility was calculated from plotting a calibration curve using regression analysis of standards and interpolating the saturation solubility of the test compounds from the calibration curve.[15]

In order to increase the aqueous solubility of the parent piperazine class, we replaced one aryl group (PhR^1) of the benzhydryl moiety with either an N-methylpiperidinyl or piperidinyl group while retaining the second aryl group (PhR^2; Table 4). The piperidinyl derivatives were synthesized from the corresponding phenyl (pyridinyl-4-yl) methanol using methodology similar to Scheme 1. The synthetic route used for the piperidinyl derivatives is presented in Scheme 2. As described in the literature,[13] phenyl (piperidin-4-yl) methanol was prepared by activating with thionyl chloride and then reacting with Boc-piperazine. The *t*-butoxycarbonyl protecting group of the product was cleaved with TFA. The deprotected amine was coupled with 3,3-diphenylpropionic acid to yield the target compounds (Scheme 2).

The activity of compounds from this series is presented in Table 4. Compound **42**, the 4-piperidinyl isomer with no substituent on the nitrogen showed good N-type blocking activity (est. IC_{50} = 0.06 μM) while the N-methylated analogue **43** was an order of magnitude less potent (est. IC_{50} = 0.69 μM). Examining further N-methylated piperidinyls (compounds **43**–**46**) showed that compounds **45** and **46** with an electron-withdrawing mono-substitution on one of the phenyl rings to be potent N-type blockers. Eliminating the phenyl group while retaining a piperidinyl group was detrimental towards maintaining N-type channel blocking affinity (compounds **47**–**49**; Table 4).

Compounds **2**, **4**–**8**, **21** and **46** were subject to in vivo assay for analgesic activity following oral dosing (Table 5). The compounds

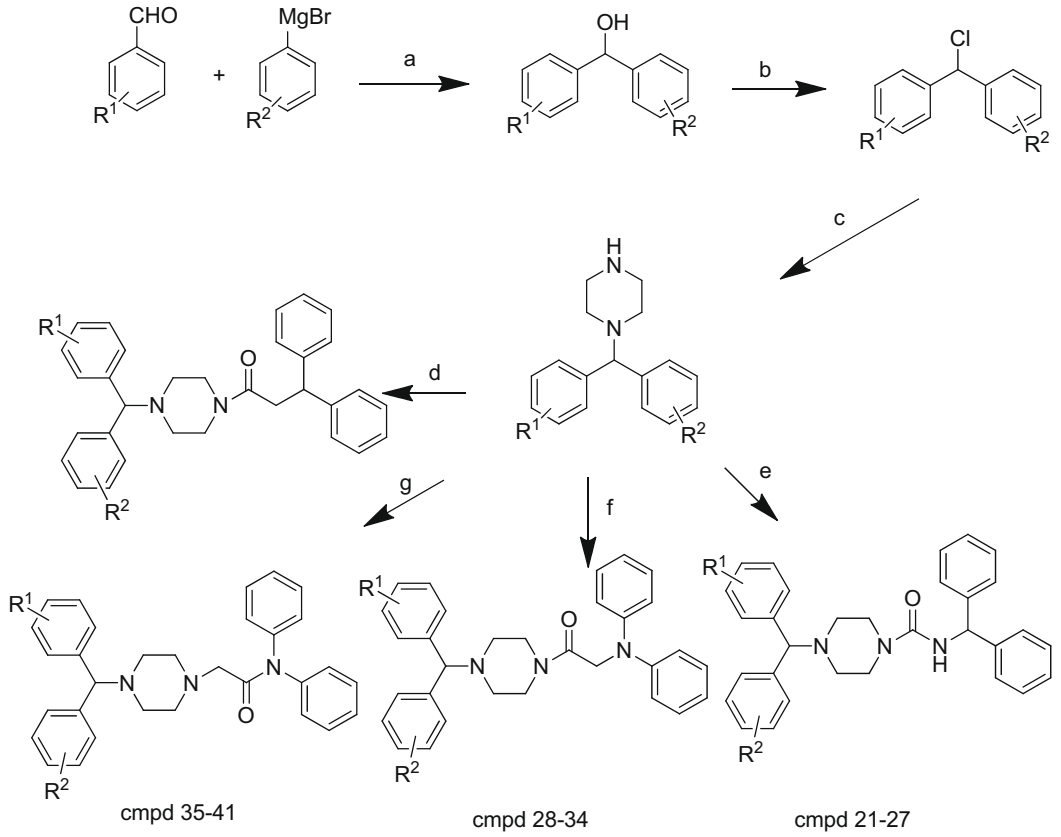

Scheme 1. Reagents and conditions: (a) ether, reflux; (b) $SOCl_2$, benzene, reflux; (c) anhydrous piperazine, K_2CO_3, KI, CH_3CN, reflux; (d) 3,3-diphenylpropanoic acid, EDC, DMAP, rt; (e) diphenylmethyl isocyanate, rt; (f) 2-(diphenylamino)acetic acid, EDC; (g) 2-bromo-*N*,*N*-diphenylacetamide, $NaHCO_3$, CH_3CN, reflux.

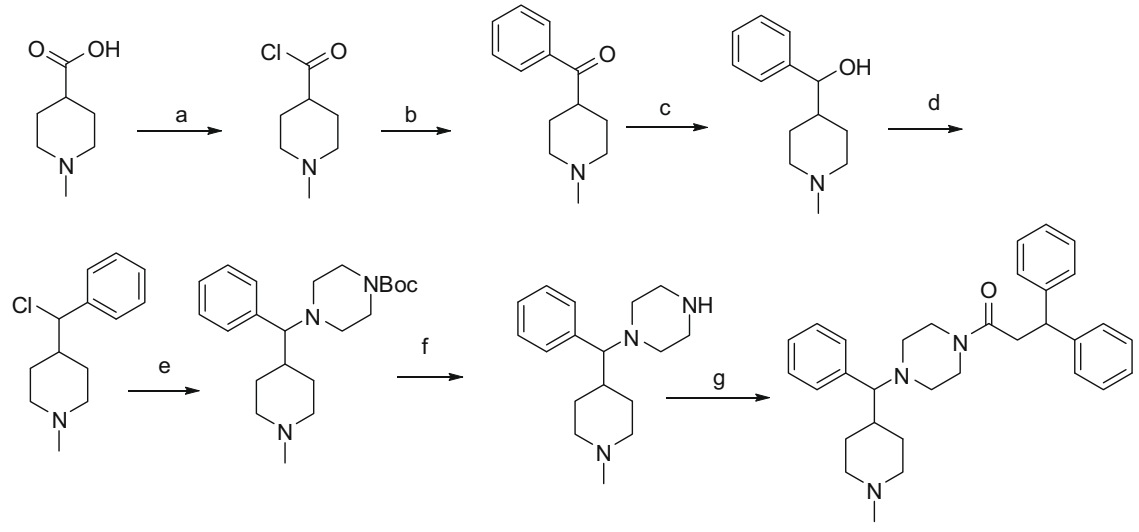

Scheme 2. Reagents: (a) $SOCl_2$; (b) $AlCl_3$, benzene; (c) $NaBH_4$, CH_3OH; (d) $SOCl_2$; (e) 4-Boc-piperazine, K_2CO_3, CH_3CN; (f) TFA, CH_2Cl_2; (g) 3,3-diphenylpropanoic acid or its derivative, EDC, DMAP, CH_2Cl_2.

were tested at a single 30 mg/kg oral dose in the Chung model of neuropathic pain with two behavioral endpoints used: mechanical allodynia and thermal hyperalgesia.[14] In both pain assessments, animals were tested at multiple intervals during a 3 h test period beginning 30 min after test compound administration. One-way ANOVA followed by the Bonferroni test were employed on the original raw data (not normalized) to establish the statistical significance of the differences observed with the baseline value. Data were normalized and expressed as means ± standard errors (SE). Compounds **5**–**8** and **21** all showed inhibition of nerve ligation-induced thermal hyperalgesia (ranging from ~45% to 98% maximal inhibition; Table 5). There did not appear to be a linear correlation between in vitro blocking activity against the N-type channel and analgesic effects in vivo (e.g., compounds **2** and **4**). Further, only two of the compounds, **5** and **21**, exhibited significant anti-allodynic effects in vivo. While compound **46** exhibited high N-type channel affinity, selectivity over the L-type channel and improved aqueous solubility compared to compounds **5** and **21**, it did not

Table 4
N-type and L-type calcium channel blocking activities for compounds **42–49**

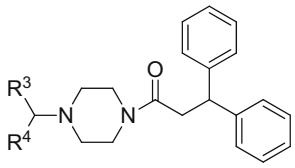

Compound	R^3	R^4	N-type IC_{50} (μM)	L-type Est. IC_{50} (μM)	L-type FLIPR IC_{50} (μM)
42	Phenyl	4-Piperidinyl	0.06		—
43	Phenyl	4-*N*-Methyl piperidinyl	0.69	100	>10
44	Phenyl	3-*N*-Methyl piperidinyl	0.27		9.3
45	4-Cl-phenyl	4-*N*-Methyl piperidinyl	0.04		3.1
46	4-F-phenyl	4-*N*-Methyl piperidinyl	0.10	11	—
47	H	4-Piperidinyl	2.5		≫10
48	H	2-Piperidinyl	2.7		—
49	H	4-*N*-Methyl piperidinyl	2.4	30	≫10

The N-type and L-type IC_{50} columns indicate estimated IC_{50} values as determined by whole-cell patch clamp of transiently expressed calcium channel complexes. For the L-type FLIPR-based assay IC_{50} values were calculated from an 8 point concentration-dependent response profile for each compound (0.003–10 μM). In those instances wherein the highest concentration (10 μM) resulted in incomplete blockade we indicate >10: 10–50% inhibition at 10 μM and ≫10 μM: less than 10% inhibition at 10 μM.

Table 5
Efficacy of compounds in the rat spinal nerve ligation model following oral dosing

Compound	Oral dose (mg/kg)	Mechanical allodynia max % activity at 60–90 min (mean ± SE)	Thermal hyperalgesia max % activity at 60–90 min (mean ± SE)
NP118809	30	80.3 ± 9.0 (p <0.001)	96.3 ± 3.7 (p <0.001)
2	30	2.6 ± 1.6 (p <0.001)	24.2 ± 12.1 (p <0.001)
4	30	ND	13.7 ± 4.5 (p <0.001)
5	30	40.2 ± 15.9 (p <0.001)	67.6 ± 10.9 (p <0.001)
6	30	3.1 ± 6.3 (p <0.001)	45.4 ± 9.9 (p <0.001)
7	30	27.6 ± 3.0 (p <0.001)	95.1 ± 4.9 (p <0.01)
8	30	27.6 ± 3.0 (p <0.001)	89.5 ± 10.5 (p <0.001)
21	30	80.9 ± 13.3 (p <0.001)	97.9 ± 2.1 (p <0.01)
46	30	ND	14.9 ± 7.7 (p <0.001)

For administration compounds were dissolved in 3 ml/kg propylene glycol and compounds administered orally (n = 5–7 animals each). Thermal hyperalgesia and mechanical hypersensitivity were measured at 30 min intervals following oral administration as described.[14] The percentage responses noted reflect the maximum activity values from baseline to the last time point examined (120 min). ND: not detected.

Table 6
Mean pharmacokinetic parameters in rat plasma following single oral or intravenous dosing for compounds **2**, **7** and **21**

Compound/route	Dose (mg/kg)	C_{max} (nM)	T_{max} (h)	$AUC_{(0-24)}$ (nM h)	$t_{1/2}$ (h)	F (%)
Compd **2** intravenous	2	2540	NA	1442	5	NA
Compd **2** oral	10	518	5	4670	4	65
Compd **7** intravenous	2	2549	NA	1602	8	NA
Compd **7** oral	10	582	3	5305	6	66
Compd **21** intravenous	2	2933	NA	2499	11	NA
Compd **21** oral	10	292	2	2785	6	22

Data are from 2 to 3 animals each and presented as the mean.
$AUC_{(0-24)}$: area under the plasma concentration versus time curve from time zero to 24 h post-dose.
C_{max}: the highest observable concentration.
T_{max}: time to C_{max}.
$t_{1/2}$: terminal elimination half-life.
F: oral bioavailability.
NA: not applicable.

show appreciable efficacy in either measure of analgesia in the SNL model. Taken together, a subset of newly discovered orally administered high affinity N-type antagonists attenuate neuropathic pain although N-type blocking affinity alone cannot predict in vivo efficacy.

In order to ascertain whether general pharmacokinetic characteristics could account in part for the differential in vivo affects observed, representative compounds were selected for profiling in rats (Table 6). Compound **2** was well absorbed orally ($C_{max} \sim 275$ ng/ml; bioavailability = 65%), albeit relatively slowly ($T_{max} \sim 5$ h) thus pain responses typically measured 1–3 h post-dosing would likely not have reflected the optimal parameters for assessing this particular agent. Comparatively, compound **7** was absorbed more rapidly ($T_{max} \sim 3$ h) and exhibited good bioavailability ($F \sim 66\%$) and half-life (~6 h). Compound **21**, which exhibited the best overall pain efficacy profile across both mechanical and thermal assessments, exhibited favorable T_{max} (~2 h) and elimination ($t_{1/2} \sim 6$ h) although bioavailability was the lowest of the compounds examined ($F \sim 22\%$). All three compounds exhibit high affinity in vitro block of the N-type channel target (IC_{50} values ~ 40–150 nM), good selectivity over the L-type channel, plasma exposures that exceed the N-type target ($C_{max} \sim 292$–518 nM), similar aqueous solubility (Table 3) and other favorable properties such as metabolic stability in rat plas-

ma (77–91% remaining at 60 min; not shown). In these regards, and taken together with our previous report,[6] it is becoming evident that direct correlations cannot be reliably made between in vitro N-type channel blocking affinity and efficacy in neuropathic and inflammatory pain models. We hypothesize that a combination of N-type affinity, physiochemical and pharmacokinetic properties together with the underlying mechanism of N-type channel blockade by each compound (e.g., state- and frequency-dependence) likely combine to determine efficacy in pain states.

In summary, optimization and structure–activity relationship studies on **NP118809** have identified potent N-type calcium channel inhibitors with good selectivity against L-type calcium channels. These studies have clarified in vitro structure–activity requirements for such agents. Compounds **5** and **21** are identified as potent orally available N-type calcium channel blockers that are ~12–86-fold selective over L-type calcium channels and exhibit mechanical and thermal analgesic activity in the rat spinal nerve ligation model.

Acknowledgements

We thank Molly Fee-Maki for helpful discussions concerning the rat PK data. Work in the laboratories of T.P.S. and G.W.Z. is supported by the Canadian Institutes of Health Research. T.P.S. a Canada Research Chair in Biotechnology and Genomics-Neurobiology. G.W.Z. is a Scientist of the Alberta Heritage Foundation for Medical Research and is also supported by a Canada Research Chair in Molecular Neurobiology.

References and notes

1. (a) Maggi, C. A.; Giuliani, S.; Santicioli, P.; Tramontana, M.; Meli, A. *Neuroscience* **1990**, *34*, 243; (b) Dubel, S. J.; Starr, T. V. B.; Hell, J.; Ahlijanian, M. K.; Enyeart, J. J.; Catterall, W. A.; Snutch, T. P. *Proc. Natl. Acad. Sci. U.S.A.* **1992**, *89*, 5058; (c) Westenbroek, R. E.; Hell, J. W.; Warner, C.; Dubel, S. J.; Snutch, T. P.; Catterall, W. A. *Neuron* **1992**, *9*, 1099; (d) Santicioli, P.; Del Biaanco, E.; Tramontana, M.; Geppetti, P.; Maggi, C. A. *Neurosci. Lett.* **1992**, *136*, 161; (e) Dunlap, K.; Luebke, J. I.; Turner, T. J. *Trends Neurosci.* **1995**, *18*, 89; (f) Evans, A. R.; Nicol, G. D.; Vasko, M. R. *Brain Res.* **1996**, *712*, 265.
2. (a) Bourinet, E.; Soong, T.-W.; Stea, A.; Snutch, T. P. *Proc. Natl. Acad. Sci. U.S.A.* **1996**, *93*, 1486; (b) Patil, P. G.; de Leon, M.; Reed, R. R.; Dubel, S. J.; Snutch, T. P.; Yue, D. T. *Biophys. J.* **1996**, *71*, 2509; (c) Zamponi, G. W.; Bourinet, E.; Nelson, D.; Nargeot, J.; Snutch, T. P. *Nature* **1997**, *385*, 442; (d) Zamponi, G. W.; Snutch, T. P. *Proc. Natl. Acad. Sci. U.S.A.* **1998**, *95*, 4035.
3. (a) Kerr, L. M.; Filloux, F.; Olivera, B. M.; Jackson, H.; Wamsley, J. K. *Eur. J. Pharmacol.* **1998**, *146*, 181; (b) Vanegas, H.; Schaible, H.-G. *Pain* **2000**, *85*, 9; (c) Wang, Y.-X.; Pettus, M.; Gao, D.; Phillips, C.; Bowersox, S. S. *Pain* **2000**, *84*, 151; (d) Staats, P. S.; Yearwood, T.; Charapata, S. G.; Presley, R. W.; Wallace, M. S.; Byas-Smith, M.; Fisher, R.; Bryce, D.; Mangieri, E. A.; Luther, R. R.; Mayo, M.; McGuire, D.; Ellis, D. *J. Am. Med. Assoc.* **2004**, *291*, 63; (e) Jain, K. K. *Expert Opin. Invest. Drugs* **2000**, *9*, 2403; (f) Bowersox, S.; Tich, N.; Mayo, M.; Luther, R. *Drugs Future* **1998**, *23*, 152.
4. Snutch, T. P. *NeuroRx* **2005**, *2*, 662.
5. (a) Hu, L.-Y.; Ryder, T. R.; Rafferty, M. F.; Cody, W. L.; Lotarski, S. M.; Miljanich, G. P.; Millerman, E.; Rock, D. M.; Song, Y.; Stoehr, S. J.; Taylor, C. P.; Weber, M. L.; Szoke, B. G.; Vartanian, M. G. *Bioorg. Med. Chem. Lett.* **1999**, *9*, 907; (b) Hu, L.-Y.; Ryder, T. R.; Nikam, S. S.; Millerman, E.; Szoke, B. G.; Rafferty, M. F. *Bioorg. Med. Chem. Lett.* **1999**, *9*, 1121; (c) Knutsen, L. J.; Hobbs, C. J.; Earnshaw, C. G.; Fiumana, A.; Gilbert, J.; Mellor, S. L.; Radford, F.; Smith, N. J.; Birch, P. J.; Ward, S. D.; Russell Burley, J.; James, I. F. *Bioorg. Med. Chem. Lett.* **2007**, *17*, 662; (d) Yamamoto, T.; Niwa, S.; Iwayama, S.; Koganei, H.; Fujita, S.; Takeda, T.; Kito, M.; Ono, Y.; Saitou, Y.; Takahara, A.; Iwata, S.; Yamamoto, H.; Shoji, M. *Bioorg. Med. Chem. Lett.* **2006**, *14*, 5333.
6. Zamponi, G. E.; Feng, Z. P.; Zhang, L.; Pajouhesh, H.; Ding, Y.; Belardetti, F.; Pajouhesh, H.; Dolphin, D.; Mitscher, L. A.; Snutch, T. P. *Bioorg. Med. Chem. Lett.* **2009**, *19*, 6467.
7. (a) Jarugu Narasimha, M.; Subhas, S. *J. Org. Chem.* **2007**, *75*, 9786; (b) Tan, E. S.; Miyakawa, M.; Bunzow, J. R.; Grandy, D. K.; Scanlan, T. S. *J. Med. Chem.* **2007**, *50*, 2787; (c) Denegri, B.; Kronja, O. *J. Org. Chem.* **2007**, *72*, 8427.
8. (a) Pajouhesh, H.; Snutch, T. P.; Zamponi, G. W.; Pajouhesh, H., Belardetti, F. U.S. Patent 6951,862, 2007.; (b) Pajouhesh, H.; Snutch, T. P.; Zamponi, G. W.; Pajouhesh, H., Belardetti, F. U.S. Patent 2004/0147529, 2004.; (c) Pajouhesh, H.; Snutch, T. P.; Pajouhesh, H., Ding, Y. U.S. Patent, U.S. 2006/0063775, 2006.; d Pajouhesh, H.; Snutch, T. P.; Ding, Y.; Pajouhesh, H. WO 2005/097779 A1, 20 Oct. 2005.; (e) Pajouhesh, H.; Snutch, T. P.; Ding, Y.; Pajouhesh, H. WO 2006/024160 A1, 9, March 2006.
9. Bourinet, E.; Soong, T.-W.; Sutton, K.; Slaymaker, S.; Mathews, E.; Monteil, A.; Zamponi, G. W.; Nargeot, J.; Snutch, T. P. *Nat. Neurosci.* **1999**, *2*, 407.
10. Snutch, T. P.; Tomlinson, W. J.; Leonard, J. P.; Gilbert, M. M. *Neuron* **1991**, *7*, 45.
11. Testing compounds for blockade of N-type and L-type calcium channels was performed by whole-cell patch clamp analysis using a near half-maximal concentration of compound applied to HEK cells transiently expressing each particular type of cloned calcium channel complex (N-type: $Ca_V2.2/\alpha_{1B} + \alpha_2\delta\text{-}1 + \beta_{1b}$ subunits; L-type: $Ca_V1.2/\alpha_{1C} + \alpha_2\delta\text{-}1 + \beta_{1b}$ subunits). Pipettes (in the range of 2–4 MΩ) were filled with internal solution containing 108 mM Cs-methanesulfonate, 4 mM $MgCl_2$, 9 mM EGTA, 9 mM HEPES (pH 7.2 adjusted with TEA-OH). Whole-cell barium currents were recorded using an Axopatch 200B amplifier and an extracellular recording solution comprised of 5 mM $BaCl_2$, 1 mM $MgCl_2$, 10 mM HEPES, 40 mM TEACl, 10 mM glucose, 97.5 mM CsCl (pH 7.2 adjusted with TEA-OH). Data were filtered at 1 kHz using a 4 pole Bessel filter and digitized at a sampling frequency of 2 kHz. Whole-cell barium current inhibition was measured from a holding potential of −100 mV to a test potential of +10 mV. The IC_{50} value was then calculated by rearranging the Michaelis–Menton equation such that $IC_{50} = [D]/((1/fr) - 1)$ where [D] is the drug concentration, and fr is the fraction of current remaining after drug application. This analysis assumes that there is a 1:1 interaction between the drug and the channel. The term 'estimated IC_{50}' is utilized since the determination of IC_{50} via a single concentration point may be slightly less accurate than fits to entire concentration-dependent response curves.
12. For higher throughput FLIPR-based screening for L-type channel blockade, HEK cells stably co-expressing the $Ca_V1.2$ L-type calcium channel complex and Kir2.3 K^+ channel were loaded with the fluorescent indicator dye, Fluo-4 (Invitrogen), and incubated for 45 min at 29 °C in 5% CO_2. After removal of excess Fluo-4 cells in buffer containing in mM: 110.5 NaCl, 10 HEPES, 10 D-glucose, 1 $CaCl_2$, 30 mM KCl (pH adjusted to 7.4 with NaOH) compounds were tested with an 8 point concentration-dependent response profile (0.003–10 μM) generated by evoking calcium entry with addition of 130 mM KCl stimulation buffer (in mM: 10.5 NaCl, 10 HEPES, 10 D-glucose, 1 $CaCl_2$, 130 KCl, pH 7.4 adjusted with NaOH). A change in the Fluo-4 fluorescence signal was assessed using FLIPR Tetra™ instrument (Molecular Devices, Sunnyvale, CA) for 3 min following the elevation of extracellular KCl using an illumination wavelength of 470–495 nm with emissions recorded at 515–575 nm. Concentration-dependent response curves were obtained by comparing the fluorescence signal increase in the presence of compound to control substances and fitted with a logistic function to obtain the concentration that inhibited 50% (IC_{50}) of the RLU signal using OriginPro v.7.5 software (OriginLab, Northampton, MA). Given the nature of the L-type channel FLIPR assay, the resulting IC_{50} values reflect blockade of channels in the partially inactivated state. In comparison, data obtained from the L-type channel whole-cell patch clamp analyses reflects open/closed state blockade. Selectivity ratios as stated in the text derive from direct comparison of N-type and L-type whole-cell patch clamp data.
13. (a) Orjales, A.; Mosquera, R.; Toledo, A.; Pumar, M. C.; Garcia, N.; Cortizo, L.; Labeaga, L. *J. Med. Chem.* **2003**, *46*, 5512; (b) Strupczewski, J. T.; Allen, R. C.; Gardner, B. A.; Schmid, B. L.; Stache, U.; Glamkowski, E.; Jones, M. C.; Ellis, D. B.; Huger, F. P.; Dunn, R. W. *J. Med. Chem.* **1985**, *28*, 761.
14. Spinal nerve ligation (SNL) injury was performed according to the method described by Kim and Chung (Kim, S. H.; Chung, J. M. *Pain,* **1992**, *50*, 355.). Male Sprague-Dawley rats (200–300 g) were maintained in a climate-controlled room on a 12 h light/dark cycle with free access to food and water until the time of the experiment. Rats were anesthetized with 2% halothane in O_2 delivered and the skin over the caudal lumbar region incised and the muscles retracted. The L_5 and L_6 spinal nerves were exposed and tightly ligated with 4-0 silk suture distal to the dorsal root ganglion. Sham-operated animals were prepared in an identical fashion except that the L_5/L_6 spinal nerves were not ligated. Thermal hyperalgesia was assessed by the method of Hargreaves and colleagues (Hargreaves, K.; Dubner, R.; Brown, F.; Flores, C.; Joris, J. *Pain* **1988**, *32*, 77.) and mechanical hypersensitivity was determined by measuring the paw withdrawal threshold in response to probing with von Frey filaments (Ossipov, M. H.; Lopez, Y.; Nichols, M. L.; Bian, D.; Porreca, F. *Neurosci. Lett.* **1995**, *199*, 87.). After baseline assessment compound or vehicle were administered by the oral route (30 mg/kg in 3 ml/kg propylene glycol) and behavioral assessments performed at 30 min intervals post-administration. The percentage activity and the difference between the contralateral and ipsilateral paws were assessed by ANOVA-post-hoc for statistic calculation. The following formula was used to calculate the % anti-allodynic activity: 100% × [(paw withdrawal thresholds after drug treatment − postSNL baseline paw withdrawal thresholds)/(preSNL baseline paw withdrawal thresholds − postSNL baseline paw withdrawal thresholds). The following formula was used to calculate the % anti-hyperalgesic activity: 100% × [(paw withdrawal latencies after drug treatment − postSNL baseline paw withdrawal latencies)/(preSNL baseline paw withdrawal latencies − postSNL baseline paw withdrawal latencies). All surgeries and behavioral testing were performed in accordance with the policies and recommendations of the International Association for the Study of Pain and the National Institutes of Health guidelines for the handling and use of laboratory animal and were approved by the Animal Care and Use Committee of the University of Arizona.
15. Test No. 105: Water Solubility, *Organization for Economic Co-Operation and Development (OECD) Guidelines for the Testing of Chemicals*, Section 1: Physical and Chemical Properties, 1995.